Non-rigid Motion Estimation Using the Robust Tensor Method

K. Palaniappan
Multimedia Communications and Visualization Laboratory
Department of Computer Science
University of Missouri-Columbia
Columbia, MO 65211
palaniappank@missouri.edu,

Hai S. Jiang
Multimedia Communications and Visualization Laboratory
Department of Computer Science
University of Missouri-Columbia
Columbia, MO 65211
hai@meru.rnet.missouri.edu

Tobias I. Baskin
Biology Department
University of Massachusetts
611 N. Pleasant St.
Amherst, MA 01003
baskin@bio.umass.edu

Abstract

This paper presents a new technique that couples tensor based image flow with robust statistical estimation models to produce dense accurate velocity fields. The 3D orientation structure tensor of the spatiotemporal varying light intensity field is used to estimate local non-rigid image motions. Previous work has shown that in highly uniform regions that lack salient corner and edge information or with noisy measurements the structure tensor approach can lead to spurious velocity estimates. The proposed algorithm improves estimates of the deformable image flow in these regions by minimizing a robust tensor functional that includes regularization and penalty terms. The robust tensor functional explicitly incorporates a temporal photometric consistency term. The combined robust tensor method is formulated as a global constrained optimization over the 3D spatiotemporal light intensity volume and recovers scientifically accurate velocity fields. An attractive aspect of the robust tensor method is simultaneous segmentation and velocity estimation. Experimental results using image sequences of biological motion captured using a calibrated video microscope reveals new biophysical insights at subcellular micron scale resolutions.

1. Introduction

The orientation or structure tensor method for estimating optical flow has been shown to provide superior motion fields in comparison to earlier methods [36],[41],[23],[22],[35]; some of the optical flow literature is reviewed in Section 5. However, the tensor method does not give reliable results when the tensor matrix is singular, or when the eigenvectors are not one of the ideal cases. Compared to these previous results for the computational estimation of image flows arising from non-rigid motions, this paper has several new contributions including: 1) an additional robust matching stage for extremely high accuracy as is needed in bioimaging applications where one-tenth of a pixel motion accuracy is required, 2) motion interpolation to fill-in areas of unreliable motion estimation for which we use a new extension to anisotropic diffusion with several weight matrices, 3) the use of an energy minimization functional that includes a forward-backward consistency term, 4) the use of auto-segmentation using motion coherence and consistency to speed up the estimation process, and 5) the use of an explicit non-rigid motion (tissue growth) model to handle spatiotemporal motion aliasing during video acquisition.

We use the orientation tensor-based optical flow estimate as an initialization for an energy minimization procedure that includes robust error functions to mitigate the impact of outliers. The tensor-based flow field is used to automatically segment the motion field to improve accuracy. A temporal photometric consistency test is used to remove unreliable optical flow estimates in the presence of deformations. The proposed algorithm has been compared and shown to be superior to manual matching methods and other image flow estimation algorithms, and experimentally validated on hundreds of real root image stacks at several different institutions.

Our proposed approach is very useful especially for bioimaging applications which may lack rich texture and have background noise motion fields that are "uninteresting" such as water rims, dust particles, intracelluluar fluid circulation, and varying imaging conditions as the biological samples are moved to acquire a complete high resolution image sequence of a tissue sample. When the texture is not sufficiently rich, pure matching methods produce erroneous or noisy results. On the other hand, the tensor method by itself is a derivative-based method, which is sensitive to noise as noted in the literature. The proposed robust tensor method is able to obtain very accurate motion fields for biological growth velocity profiles that are in the range of 0.05 to 0.13 pixel per second (over a nine frame sequence) at a scale of one micron per pixel that has been validated manually by domain experts. The unprecedented spatial and temporal resolution in determining the deformable motion profiles have led to new biological insights about cellular growth under different environmental and physiological conditions that was previously not possible [52].

Proceedings of the 2004 IEEE Computer Society Conference on Computer Vision and Pattern Recognition Workshops (CVPRW'04)
1063-6919/04 $ 20.00 IEEE

The motivation for this research was to quantitatively describe biological growth and motility, which involve nonrigid motion processes. This is an important aspect of characterizing the biophysical and genetic makeup of an organism's function, phenotype and disease processes. This paper develops the robust tensor non-rigid motion estimation algorithm for accurately measuring the growth profile of biological tissues at the subcellular scale. Organisms grow throughout their lives and their many physiological behaviors are based on growing new organs with different shapes or properties. Quantitative methods of motion estimation would be useful for bridging the gap between genotype and phenotype especially when coupled to microarray studies of gene expression and proteomics. That is quantitative motion can be used in rapidly characterizing or screening the affects of genetic modification studies to select organisms for environmental response to water stress, salt stress, metal ion stress, insect stress, pesticide resistance, etc.

2. 3D Structure Tensor Orientation-based Velocity Fields

The robust tensor algorithm combines tensor-based image flow [35],[22],[23] with robust matching [13],[51] and motion field interpolation to estimate velocity fields densely and accurately. We first describe the fast orientation tensor based deformable image flow estimation process.

An image sequence can be considered as a spatiotemporal image volume of light intensities or gray levels. Using the spatiotemporal volume explicitly enables the treatment of velocity or displacement vector field estimation as a geometric 3D orientation estimation problem based on the local volume of gray values.

Consider an image sequence as a spatio-temporal volume of gray levels. Assuming image brightness is conserved, which is strictly valid only for rigid motion, leads to the continuity equation:

$$\frac{dI(\mathbf{x})}{dt} = 0 = \frac{\partial I(\mathbf{x})}{\partial x} v_x(\mathbf{x}) + \frac{\partial I(\mathbf{x})}{\partial y} v_y(\mathbf{x}) + \frac{\partial I(\mathbf{x})}{\partial t} = \nabla I(\mathbf{x}) \bullet \mathbf{v}(\mathbf{x}) \quad (1)$$

where $I(\mathbf{x}) = I(x,y,t)$, $\mathbf{v}(\mathbf{x}) = \begin{pmatrix} v_x(\mathbf{x}) & v_y(\mathbf{x}) & 1 \end{pmatrix}^T$ is the spatio-temporal volume of image gray levels and motion vectors respectively. This equation is also known as the image flow or optical flow equation and is often derived from the first order terms in a Taylor series representation of $I(\mathbf{x})$ within a local neighborhood around $\mathbf{x}$. The continuity equation states that the spatio-temporal motion field is everywhere locally orthogonal to the spatio-temporal gradient of the signal or image stack. In addition to brightness constancy, illumination constancy is also required to relate image flow to object motion. The image flow equation provides one constraint on the flow vector, which has two unknowns.

The estimation of the velocity or displacement vector field based on the local spatio-temporal volume of light intensities can be treated as the local estimation of geometric 3D orientation. Since the motion vector, $\mathbf{v}$, should be orthogonal to all the gray value gradients within a spatio-temporal neighborhood η we are interested in estimating $\mathbf{v}$ that minimizes in a least squares sense the expression:

$$S = \int_{\eta} \left(\nabla I(\mathbf{x}) \bullet \mathbf{v}(\mathbf{x}) \right)^2 d\mathbf{x}' \quad (2)$$

The minimization, Eq 2, can be written in matrix form as:

$$S = \mathbf{v}^T \mathbf{J} \mathbf{v}, \ with \ \mathbf{J}(\mathbf{x}) = \int_{-\infty}^{+\infty} w(\mathbf{x} - \mathbf{x}') \nabla I(\mathbf{x}') \nabla I^T(\mathbf{x}') d\mathbf{x}' \quad (3)$$

The 3 x 3 symmetric structure-tensor matrix, $\mathbf{J}(\mathbf{x})$, based on the local spatio-temporal volume of gray values has components, J_{pq}, given by:

$$J_{pq} = \int_{-\infty}^{+\infty} w(\mathbf{x} - \mathbf{x}') \frac{\partial I(\mathbf{x}')}{\partial x_p} \frac{\partial I(\mathbf{x}')}{\partial x_q} d\mathbf{x}' \quad (4)$$

$$\sum_{\substack{3d \ neiborhood \ centered \\ at \ the \ pixel \ DD[t][x][y]}} Dx[t][x][y] * Dx[t][x][y]$$

where $I(\mathbf{x}) = I(x,y,t)$ is the spatiotemporal volume of light intensities or image gray levels, $\partial I(\mathbf{x}') / \partial x_p$ is the partial derivative of the spatio-temporal volume along the x_p axis direction, and $d\mathbf{x}' \equiv dx \cdot dy \cdot dt$ specifies a volume integration [12],[37],[38],[46],[35],[27]. The window function $w(\mathbf{x} - \mathbf{x}')$ defines the weighted neighborhood (local area and time) over which the inertia or structure-tensor is computed. The window function filters the spatio-temporal derivative estimates and critically affects performance by conditioning the structure-tensor matrix. The 3x3 symmetric structure-tensor is given by:

$$\mathbf{J} = \begin{bmatrix} J_{xx} & J_{xy} & J_{xz} \\ J_{yx} & J_{yy} & J_{yz} \\ J_{zx} & J_{zy} & J_{zz} \end{bmatrix} \approx \begin{bmatrix} \sum_{\eta} D_x D_x & \sum_{\eta} D_x D_y & \sum_{\eta} D_x D_t \\ \sum_{\eta} D_x D_y & \sum_{\eta} D_y D_y & \sum_{\eta} D_y D_t \\ \sum_{\eta} D_x D_t & \sum_{\eta} D_y D_t & \sum_{\eta} D_z D_t \end{bmatrix} \quad (5)$$

and can be approximated using a weighted average of local discrete derivatives, D_{x_p}, within the neighborhood η in the direction x_p as shown in Eq. 5. The vector $\mathbf{v}(\mathbf{x})$ that minimizes Eq. 3 is the eigenvector of tensor J corresponding to the smallest eigenvalue. So when the local image or optic flow can be assumed to be an accurate indication of the local velocity field then the estimation of local orientation in the spatio-temporal volume can be shown to be equivalent to an eigenvalue analysis of the structure tensor [32],[46].

The structure tensor approach is versatile for computing low-level motion since it is independent of explicit image matching, feature tracking, or exhaustive search. Other strengths of the tensor approach are that it

uses only first order derivative information that is more simpler than higher order derivative estimation, is unbiased by white Gaussian noise, is not sensitive to gradual changes in velocity, can be readily extended to multidimensional signals (i.e. 4D structure tensor for timevarying volumetric data) and facilitates fusion of displacement vectors from multispectral or multichannel images. The tensor method can incorporate global illumination changes that violate the brightness constancy assumption [31] but is sensitive to motion discontinuities or large motion. A locally varying affine motion model is used to model **v(x)** the deforming flow field as accurately as possible.

3. Robust Estimation

A mathematical technique is needed to reduce the negative influence of gross errors or outliers in the optimization process to improve the reliability of the estimate. Robust statistics provides such a framework for automatically restricting the effects of outliers [47]. For example, the sample median is a robust estimator whereas the sample mean is very sensitive to outliers. Similarly, optimization or regression methods using least sum of squares have a breakdown point of 1/n for n observations whereas using least median of squares has a breakdown point of 50% [47]. The breakdown point is the percent of outliers that will cause the estimator to change without bound. The Geman-McClure robust estimator function or influence function, $\rho_i(x,\sigma_i) = x^2/\left(x^2+\sigma_i^2\right)$, saturates at one for large values of x. Hence outliers in the motion field only have a negligible effect on the local velocity estimate. This enables the robust-tensor method to produce accurate dense motion fields even in the presence of outliers. The neighborhood size is typically 15 x 15 with a searching window size of 31 x 51 depending on the characteristics of the source images. Robust statistics for low level vision were investigated by Black and Rangarajan [15] and for estimating multiple optical flow fields by Black and Anandan [13]. An anisotropic approach that does not use robust methods to improve the tensor estimates is described in Spies and Scharr [50].

For robust matching, an energy minimization approach has been implemented that combines compatibility in local texture, spatial flow and temporal consistency. To the best of our knowledge, this robust-tensor energy minimization approach is unique. The tensor-based portion uses the 3D structure tensor of the spatio-temporally varying intensity field to estimate local image motion. Confident estimation of velocities depends on the presence of linear and point feature types of motion. Unfortunately, spurious estimation of velocity occurs where the images are noisy or in regions that lack salient corner and edge information. This is the so-called aperture problem, which is a consequence of estimating motion through finite receptive fields or windows. For example, for a moving edge with little texture, only the component of velocity perpendicular to the edge (in the gradient direction) can be estimated. Even corners will produce ambiguous motion along the edges of the corner and motion can be considered accurate only at a singular point, the corner itself. A moving edge has an ambiguous direction in the motion flow of up to 180 degrees and a corner up to 90 degrees.

The algorithm identifies low confidence image flow regions by using the eigenvalues of the structure tensor, and then makes an improved estimate of image flow in these regions. The improvement is achieved using a robust statistical estimation procedure, described below, that recovers piecewise similar, smooth, and coherent flows. The algorithm incorporates a robust penalty function to model structural changes, motion discontinuities, and temporal asymmetry.

4. Regularization Using the Robust Tensor Functional

Robust estimation is incorporated in our motion estimation algorithm as a regularized energy minimization process. The robust penalty function in Eq 6 models motion discontinuities by penalizing intensity changes, regularizing the flow field locally and enforces temporal photometric consistency (ie penalizes differences between temporal forward and temporal backward flow estimates) that works well in most regions except close to sources or sinks in the flow field. This temporal photometric consistency test is a new constraint that has not been previously used in motion estimation. The optimization leads to an image flow field that suitably decomposes non-rigid motions into a set of non-overlapping piece-wise smooth motion fields for further quantitative analysis. Higher accuracy, faster computation, and simultaneous segmentation plus optical flow estimation are achieved using the robust tensor functional.

We use a robust energy minimization approach to find the best values for velocities (u_s, v_s) that minimize an energy functional composed of three terms measuring properties about the flow field and image stack, *C*, using only the reliable tensor velocities as initial estimates. The assumption behind the robust approach is that the image and velocity fields are locally coherent when the images are matched correctly in a piecewise manner.

The robust energy minimization criterion includes three weighted positive compatibility constraints or penalty terms, shown in Eq. 6 below and used to find the optimal motion vector (u_s, v_s) at location **x**. In Eq 6 α_i are positive weights that control the relative contribution from each penalty term. The first term C_1 enforces piecewise texture and brightness compatibility with respect to the assumed motion model within the neighborhood N_1; this is a robust sum-of-squared differences constraint. The

function $\rho_i(x,\sigma_i) = x^2/(x^2+\sigma_i^2)$ is the Geman-McClure robust estimator that reduces the influence of outliers during the parameter search process and is controlled using the scale parameter σ_i. The second component C_2measures the smoothness of the velocity field using first derivatives of the *u*- and *v*- components in a local neighborhood N_2 and is often referred to as the flow regularization component.

$$\begin{aligned} C(\mathbf{x};u_s,v_s) = \alpha_1 C_1 + \alpha_2 C_2 + \alpha_3 C_3 \\ \alpha_1 \sum_{\mathbf{x}\in N_1} \left[\rho_1\left(I(x,y,t) - I(x+u_s\Delta t, y+v_s\Delta t, t+\Delta t), \sigma_1\right)\right] + \\ \alpha_2 \sum_{r\in N_2} \left[\rho_2\left(|u_s - u_r|, \sigma_2\right) + \rho_2\left(|v_s - v_r|, \sigma_2\right)\right] + \\ \alpha_3 \sum_{\mathbf{x}\in N_3} \left[\rho_3\left(\left|M_x^F(x,y,t) + M_x^B(x+u_s\Delta t, y+v_s\Delta t, t+\Delta t)\right|, \sigma_3\right) + \right. \\ \left. \rho_3\left(\left|M_y^F(x,y,t) + M_y^B(x+u_s\Delta t, y+v_s\Delta t, t+\Delta t)\right|, \sigma_3\right)\right] \end{aligned} \quad (6)$$

The third component C_3measures the error in the requirement that the forward motion flow $M_x^F(\,)$and backward flow $M_x^B(\,)$velocity fields should be odd-symmetry in time, that is:

$$M_x^F(x,y,t) \approx -M_x^B(x+u_s\Delta t, y+v_s\Delta t, t+\Delta t) \quad (7)$$

so that the motion model computed forward in time should be equal and opposite that computed backward in time using a uniform velocity model. The temporal photometric compatability constraint is valid outside of sources and sinks in the flow (ie. regions of cell production or cell collapse) when the amount of deformable motion is locally small enough. In our experiments usually the weights are equal. Spatially adaptive weights are being investigated analytically and evaluated experimentally.

A complex motion model including second-order acceleration terms can also be used in this forward-backward symmetry constraint. Additionally the requirement for temporal compatibility can be enforced by using a large penalty factor for α_3. The robust estimator, $C(\mathbf{x};u_s,v_s)$, used to find optimal velocity fields is minimized by sequential gradient search.

One unique aspect of the robust tensor approach is simultaneous segmentation and velocity estimation of an image sequence stack, and the incorporation of time symmetry in the robust estimator. Other penalty terms can be readily added to the energy minimization function as appropriate; for example, compatibility of (zero-crossing) contour-based flows [39]. Explicit segmentation of the motion field could be incorporated by using the Mumford-Shah functional [44] with explicit shape models for boundaries [17]. By adding a line or boundary process to Eq 6 extends the energy minimization functional to the form of the Mumford-Shah segmentation functional. An iterative candidate region growing approach for explicit segmentation of the tensor motion field under locally affine deformations is given in Farnebäck [23]. Iterative region growing is computationally expensive whereas the implicit segmentation provided by the robust functional is qualitatively comparable and fast. A similar approach to improving the robustness of optic flow estimates is to combine the local structure tensor method with the global Horn-Schunck smooth flow regularized minimization method [16]. The proposed approach not only uses regularized energy minimization but explicitly models outlier statistics and incorporates temporal photometric consistency terms, which improve the quantitative accuracy of the optic flow fields arising from nonrigid motion dynamics.

4.1. Anisotropic Interpolation of Sparse Velocity Fields

A normalized convolution approach is used to interpolate sparse velocity regions, as described by the following matrix equation:

$$\mathbf{Br} = \mathbf{B}\left(\mathbf{B}^*\mathbf{W}_a\mathbf{W}_c\mathbf{B}\right)^{-1}\mathbf{B}^*\mathbf{W}_a\mathbf{W}_c\mathbf{f} \quad (8)$$

where **B** is the local signal model, using for example a polynomial basis,{1, *x*, *y*, x^2, *x y*, y^2}, $\mathbf{W}_a$ is an applicability matrix or filter, $\mathbf{W}_c$, is the confidence weight matrix indicating the reliability of each velocity estimate, **f** is the local velocity field estimate, and **Br** represents the interpolated velocity field as a projection operator. The procedure is anisotropic because it is confined by the boundary set of known regions of the flow field. Interpolation proceeds iteratively outward or inward from such boundary constraints. To improve interpolation, we combine the confidence measures from the tensor and robust estimation steps (such as forward-backward matching to satisfy the time-symmetry constraint) by using either a median or max operation to estimate a more accurate confidence weight matrix, $\mathbf{W}_c$. Also, the applicability, $\mathbf{W}_a$, can be tuned using different filters such a Gaussian function with $\sigma = 1.2$, which has good orientation estimation properties. If necessary, the projection basis can be higher than second order to model perspective projection more accurately.

5. Brief Review of Optical Flow Methods

There has been extensive research done on image motion or optical flow estimation since Gibson coined the term in the 1950's. A brief background to this literature is provided. The image stack is treated as a three dimensional image volume, and spatio-temporal structures are defined within the volume. The orientation of the structure with respect to the time axis defines the velocity of movement. Structures can be defined by various mathematical means. In *optical flow* methods, the

projected image intensity distribution of a moving object or feature is assumed to be conserved [5],[8],[33]. Quantifying deformable motion is demanding because the object changes while moving. Extant algorithms take advantage of constraints that are specific to a given application, such as machine vision [3],[24],[25],[28],[34],[53],[54] graphics [20],[43], or atmospheric science [29],[45],[57]. Improving optical flow estimation algorithms to handle deformable motion is an active area in computer vision, with investigators focusing on issues such as motion grouping, registration, object tracking, transparency, multiple objects moving ballistically, and combining motion cues with other vision cues to recover 3D scene information [2],[9],[34],[49],[56].

The optical flow-based algorithms that have been applied to growth and motility can be divided roughly into three classes: parametric, tensor, and matching. Parametric methods fit an affine transformation to the motion within a region of interest [14]; this is an approximate solution because all pixels in the region are constrained to undergo the same transformation. The tensor methods are differential methods based on following intensity gradients [35]; they are computationally fast but prone to errors. Finally, matching methods find corresponding regions in a pair of images by maximizing a similarity criterion or minimizing an error criterion [7],[13],[42]. Matching methods tend to be slow, sensitive to neighborhood size, local image content, and outliers; however, they can be highly accurate, particularly when the search process incorporates robust statistics.

In studies of cell motility and growth, there are a few examples of the use of each type of algorithm [18],[19],[55]. Tracqui and co-workers have estimated motion parametrically in crawling and dividing single cells as well in as mono-layers involved in wound healing [26]. In their approach, the motion of the cell or monolayer was reduced to a single transformation and thus was appreciably simplified. Matching methods have been applied to muscle contraction in the leech as well as to the elongation of the grass seedling coleoptile [4],[6],[7],[40]. Tensor methods have been applied to cells moving in slime mold slugs and mounds but without evaluating the confidence or density of the recovered velocities. And more recently tensor methods have been applied to the growth of plant leaves [32],[48], where the relatively sparse distribution of estimated confident pixels requires extensive interpolation.

6. Experiments

In the biological application of cellular root growth that is important for understanding cell division in the meristem, the root tip about one to two mm in length is undergoing differential longitudinal expansion [21]. It should be pointed out that the important biophysical kinematic parameters of the research is to precisely and reproducibly measure spatial strain rate, cell flux, cell production and division which are the gradient of the velocity field, velocity divided by cell length, and the gradient of cell flux respectively [10],[11]. Hence the goal is derived properties of the motion field including accurate gradients and transformations of the motion field. This implies that many current methods for motion estimation have unacceptable shortcomings because they are too noisy or too sparse (ie along contours) for obtaining spatially dense and accurate cell kinematic maps. Some of the challenges in estimating deformable growth velocity fields for biological samples are due to low texture content, cytoplasmic streaming which produces high frequency motion artifacts, background media motion near the sample, and multi-image registration. The proposed method has demonstrated the capability to estimate velocities accurate in the range of 0.057 to 0.147 micron per second. Validation can be done by manual tracking using graphite markers or fluorescent probes [30].

The resulting velocity profiles are highly accurate and extremely informative for extracting quantitative biophysical parameters. Validation of the approach has been done using synthetic imagery (results not shown) and comparison with manual results and comparison with other algorithms. We use an optimized 3D Sobel filter (3 x 3 x 3) based on the derivative of a 3D Gaussian function, and an adaptive neighborhood initially 7 x 7 x 7, to compute the structure tensor. The results are shown in Figure 1 and compared with several other optical flow estimation algorithms in Figure 2. Fig 1 shows steps in the robust tensor velocity estimation algorithm. Fig 1A is one input frame from a 9 frame image stack in the middle of the root's growth zone. Scale bar = 50 μm. Fig 1B is the result of the first stage of motion estimation, showing object segmentation based on a two-step motion mask with high confidence tensor-based velocity regions colored red which can be seen to be sparse. Velocities parallel and perpendicular to the medial axis of the root are computed. Fig 1C is the pure, tensor-based velocity field which is relatively smooth but high confidence velocities are sparse. Fig 1D is the velocity field from one step of robust estimation showing the displacement field between the 1st and 9th frames (forward matching). Fig 1E is the velocity field after eliminating unreliable data with the forward-backward motion consistency test. Fig 1F is the final robust-tensor velocity field after motion interpolation. Images 1C — F are pseudocolored, as indicated in the color bar in panel F, with velocities ranging from 0 to 2.5 pixels per frame moving to the left. Figure 2 shows a comparison of our robust-tensor algorithm to two other optic flow-based motion estimation algorithms. Fig 2A is a complete robust-tensor motion field, reproduced from Fig 1. Fig 2B is the motion field produced by the Lucas and Kanade algorithm implemented in FlowJ [1] using parameters $s_s = 1.5$, $s_t = 0.83$, $t = 1$, $s_w = 1$ and Gaussian derivatives(ref). The speed ranged from –7.00 to +4.13 pixels per frame with

negative values indicating left direction. Fig 2C is the motion field produced by the Uras algorithm FlowJ implementation using parameters $s_s = 1.5$, $s_t = 0.83$, t = 1, w = 2 [52].The speed ranged from –20.00 to +20.00 pixels per frame. Fig 2D is the integrated velocity profiles along the midline for the three methods using the *same motion mask* as dervied by our robust-tensor method. The robust-tensor mask was used since the other algorithms do not provide motion segmentation. Velocity was averaged perpendicular to the midline for each motion field. A negative value indicates motion torward the left (toward the root tip) and values are reported in the laboratory coordinate system (not in the coordinate system with tip being the origin at the zeroth frame). The velocity maps in Figures 2A — C show speed parallel to the root midline (or medial axis) are pseudocolored using the color bar in panel C, with velocities ranging from 0 to 2.5 pixels per frame moving to the left.

7. Conclusions and Future Work

In summary, the combined robust tensor method is a combined global energy minimization approach with locally optimal constraint enforcement over a 3D spatio-temporal image space that recovers highly accurate velocity fields. Our initial objective to measure spatially varying velocity fields using image stacks to capture the full spatial variability of deformable motion has been achieved using a new robust tensor approach for estimating deformable flow fields. The robust tensor method has been validated for the precise quantitative estimation of spatially varying growth profiles in the root meristem. In the future we propose using fluorescent tagging of cells. This small labeled group of cells can potentially be very accurately tracked through the image stacks to create an accurate velocity profile. The fluorescent tagged velocity profile can then be quantitatively compared with the robust-tensor velocity profile for validation purposes.

8. Acknowledgements

The authors would like to thank Corine M. van der Weele and Krishnan Palaniappan for providing the video microscopy root meristem images. This research was supported in part by the U.S. National Science Foundation awards EIA 9911095 (KP), IBN 9817132 (TIB), and by the National Institutes of Health NIBIB award 1 R33 EB00573-01A1.

9. References

[1] Abràmoff MD, Niessen WJ, Viergever MA, 2000. Objective quantification of the motion of soft tissues in the orbit. *IEEE Trans. Med. Imaging* 19:986—995.

[2] Aksoy S, Ye M, Schauf ML, Song M, Wang Y. Haralick RM, Parker JM, Pivovarov J, Royko D, Sun C, Farneback G, 2000. Algorithm performance contest. *15th International Conference on Pattern Recognition*, V. 4: 870—876.

[3] Anandan P, 1989. A computational framework and an algorithm for the measurement of visual motion. *Int. J. Computer Vision* 2: 283—310.

[4] Barron JL, Liptay A, 1994. Optical flow to measure minute increments in plant growth. *BioImaging* 2: 57—61.

[5] Barron, JL, Fleet DJ, Beauchemin SS, 1994. Performance of optical flow techniques, *Int J Computer Vision*, 12: 43-77, 1994.

[6] Barron JL, Liptay A, 1997. Measuring 3D plant growth using optical flow. *BioImaging* 5: 82-86.

[7] Barron JL, Liptay A, Spies H, 2000. Optical flow and range flow for plant growth and leaf motion. In: *Image and Vision Computing 2000* (ICVNZ2000), Hamilton, New Zealand, pp. 68—77.

[8] Beauchemin SS, Barron JL, 1995. The computation of optical flow. *ACM Computing Surveys*, 27 (3): 433—467.

[9] Beauchemin SS, Barron JL, 1999. On discontinuous optical flow, *Computers Art. Intel.* 19: 255—283.

[10] Beemster GTS, Baskin TI, 1998. Analysis of cell division and elongation underlying the developmental acceleration of root growth in *Arabidopsis thaliana. Plant Physiol*ogy 116: 1515-1526.

[11] Beemster GTS, Baskin TI, 2000. STUNTED PLANT 1 mediates effects of cytokinin, but not of auxin, on cell division and expansion in the root of arabidopsis. *Plant Physiol*ogy 124: 1718—1727.

[12] Bigün J, Granlund GH, 1987. Optimal orientation detection of linear symmetry. *Proc. ICCV*, London.

[13] Black MJ, Anandan P, 1996. The robust estimation of multiple motions: parametric and piece-wise smooth flow fields. *Comput. Vision Image Understanding* 63: 75—104.

[14] Black M, Jepson AD, 1996. Estimating optical flow in segmented images using variable-order parametric models with local deformations. *IEEE Trans. Pattern Analysis Machine Intelligence*. 18. 972—986.

[15] Black MJ, Rangarajan A, 1996. On the unification of line processes, outlier rejection, and robust statistics with applications in early vision. *Int. J. Computer Vision* 19: 57—91.

[16] Bruhn A, Weickert J, Schnorr C, 2002. Combining the advantages of local and global optic flow methods. *Proc. Pattern Recognition: 24th DAGM Symposium*, Lecture Notes in Computer Science, V. 2449, pp. 454 – 462.

[17] Cremers D, Tischhäuser F, Weickert J, Schnörr C, 2002. Diffusion Snakes: Introducing statistical shape knowledge into the Mumford-Shah functional. *Int J Computer Vision*, 50(3): 295-313.

[18] Earnshaw R, Magnenat-Thalmann N, Terzopoulos D, Thalmann D, 1998. Computer animation for virtual humans. *IEEE Computer Graphics Applications*. 18: 20—23.

[19] Erickson RO, Sax KB. 1956. Rates of cell division and cell elongation in the growth of the primary root of Zea mays. *Proc. Amer. Phil. Soc*. 100: 499—514.

[20] Farnebäck G, 2000. Fast and accurate motion estimation using orientation tensors and parametric motion models. *Proc. 15th IAPR Inter. Conf. Pattern Recognition*, Barcelona, Spain.

[21] Farnebäck G, 2001. Very high accuracy velocity estimation using orientation tensors, parametric motion, and simultaneous segmentation of the motion field, *8th IEEE Int. Conf. Computer Vision*, V. 1: 171-177.

[22] Fleet DJ, Jepson AD, 1989. Hierarchical construction of orientation and velocity selective filters. *IEEE Trans. Pattern Analysis Machine Intelligence*, 11(3): 315-325.

[23] Fleet DJ, Jepson AD, 1990. Computation of component image velocity from local phase information. *Int. J. Computer Vision*, 5(1): 77-104.

[24] Germain F, Doisy A, Ronot X, Tracqui P, 1999. Characterization of cell deformation and migration using a parametric estimation of image motion. *IEEE Trans. Biomed. Engin*. 46: 584—599.

[25] Granlund G, Knutsson H, 1995. *Signal Processing for Computer Vision*. Kluwer, Dordrecht.

[26] Halevi G, Weinshall D, 1997. Motion of disturbances: detection and tracking of multi-body non-rigid motion. *Proc. IEEE Computer Vision and Pattern Recognition*, pp. 897—902.

[27] Hasler AF, Palaniappan K, Kambhammetu C, Black P, Uhlhorn E, Chesters D, 1998. "High resolution windfields within the inner core and eye of a mature tropical cyclone from GOES 1-min images", *Bulletin of the American Meteorological Society,* Vol. 79, No. 11, Nov., pp. 2483-2496.

[28] Haugland RP, 1996. *Handbook of Fluorescent Probes and Research Chemicals*, 6th Ed'n Molecular Probes, Eugene OR. pp 344-351.

[29] Haussecker HW, Fleet DJ, 2001. Computing optical flow with physical models of brightness variation. *IEEE Trans. Pattern Analysis Machine Intelligence*, 23(6):661-673.

[30] Haußecker H, Jähne B, 1997. A tensor approach for precise computation of dense displacement vector fields. In: *Proc. Mustererkennung, DAGM Symposium*, Braunschweig, Springer, pp. 199—208.

[31] Horn BKP, Schunck BG, 1981. Determining optical flow. *Artificial Intelligence.* 17: 185—204.

[32] Huang Y, Palaniappan K, Zhuang X, Cavanaugh J, 1995. "Optic flow segmentation and motion estimation using a robust genetic partitioning algorithm", *IEEE Trans. Pattern Analysis Machine Intelligence*, Vol. 17, No. 12, pp. 1177-1190, Dec. 1995.

[33] Jähne B 1997. *Practical Handbook on Image Processing for Scientific Applications* CRC Press.

[34] Jiang H, Palaniappan K, Baskin TI, 2003. A combined matching and tensor method to obtain high fidelity velocity fields from image sequences of the non-rigid motion of plant root growth", *IASTED Int. Conf. on Biomedical Engineering, BioMED 2003*, June 25-27, 2003, Salzburg, Austria.

[35] Kass M, Witkin A, 1987. Analyzing oriented patterns. *Computer Vision Graphics and Image Proc.*, 37: 362—385.

[36] Knutsson H, 1989. Representing local structure using tensors. *Sixth Scandanavian Conf. Image Analysis*, Finland, pp. 244-251.

[37] Lai SH, Vemuri BC, 1998. Reliable and efficient computation of optical flow. *Int J Computer Vision*, 29(2):87-105.

[38] Liptay A, Barron JL, Jewett T, van Wesenbeeck I, 1995. Oscillations in corn seedling growth as measured by optical-flow. *J. Amer. Soc. Hort. Sci.* 120: 379—385.

[39] Liu, H, Chellappa R, Rosenfeld A, 2003. Accurate dense optical flow estimation using adaptive structure tensors and a parametric model, *IEEE Trans. Image Processing*, 12(10):1170-1179.

[40] Lucas B, Kanade T, 1981. An iterative image registration technique with an application to stereo vision. *Proc. DARPA IU Workshop*, pp. 121—130.

[41] Metaxas D, Terzopoulos D, 1993. Shape and nonrigid motion estimation through physics-based synthesis. *IEEE Trans. Pattern Analysis Machine Intelligence*. 15: 580—591.

[42] Mumford D, J.Shah J, 1989. Optimal approximation by piecewise smooth functions and associated variational problems. *Comm. Pure Appl. Math*. 17:577–685.

[43] Palaniappan K, Kambhamettu C, Hasler AF, Goldgof DB, 1995. "Structure and semi-fluid motion analysis of stereoscopic satellite images for cloud tracking*", Fifth Int. Conf. Computer Vision*, MIT, June 20 - 23, IEEE Computer Society Press, pp. 659-665.

[44] Rao, AR, 1990. *A Taxonomy for Texture Description and Identification*. Springer, Berlin.

[45] Rousseeuw PJ, 1998. Robust estimation and identifying outliers. *Handbook of Statistical Methods for Scientists and Engineers*, 2nd Ed, HM Wadsworth (ed), Chapter 17.

[46] Schmundt D, Stitt M, Jähne B, Schurr U, 1998. Quantitative analysis of the local rates of growth of dicot leaves at a high temporal and spatial resolution, using image sequence analysis. *Plant Journal*. 16: 505—514.

[47] Seetharaman G, Gasperas G, and Palaniappan K, 2000. A piecewise affine model for image registration in 3-D motion analysis, *IEEE Int. Conf. On Image Processing*, Vancouver, BC, Canada, Sep. 10-13, pp. 561-564.

[48] Spies H, Scharr H, 2001. Accurate optical flow in noisy image sequences. *8th IEEE Int. Conf. Computer Vision*, V. 1: 587-592.

[49] Szeliski R. 1999. A multi-view approach to motion and stereo. *IEEE Conference on Computer Vision and Pattern Recognition*. IEEE Comput. Soc. V. 1, 157—163.

[50] van der Weele C, Jiang H, Palaniappan KK, Ivanov VB, K. Palaniappan, Baskin TI, 2003. "A new algorithm for computational image analysis of deformable motion at high spatial and temporal resolution applied to root growth: Roughly uniform elongation in the meristem and also, after an abrupt acceleration, in the elongation zone," *Plant Physiology*, Vol. 132, No. 3, pp. 1138-1148.

[51] Vedula S, Baker S, Seitz S, Kanade T, 2000. Shape and motion carving in 6D, *Proc. IEEE Computer Vision Patt. Recog*. 2: 592—598.

[52] Weng J, Ahuja N, Huang TS, 1987. 3-D motion estimation, understanding, and prediction from noisy image sequences. *IEEE Trans. Pattern Analysis and Machine Intelligence*. 9: 370—389.

[53] Wu K, Gauthier D, Levine MD, 1995. Live cell image segmentation. *IEEE Trans. Biomed. Engineering*. 42: 1—12.

[54] Ye M, Haralick RM, 2000. Optical flow from a least trimmed squares based adaptive approach. 15th *International Conference on Pattern Recognition*, V. 3: 1052—1055.

[55] Zhou L, Kambhammetu C, Goldgof D, Palaniappan K, Hasler AF, 2001. "Tracking non-rigid motion and structure from 2D satellite cloud images without correspondences", *IEEE Trans. Pattern Analysis Machine Intelligence*, Vol. 23, No. 11, Nov. 2001, pp. 1330-1336.

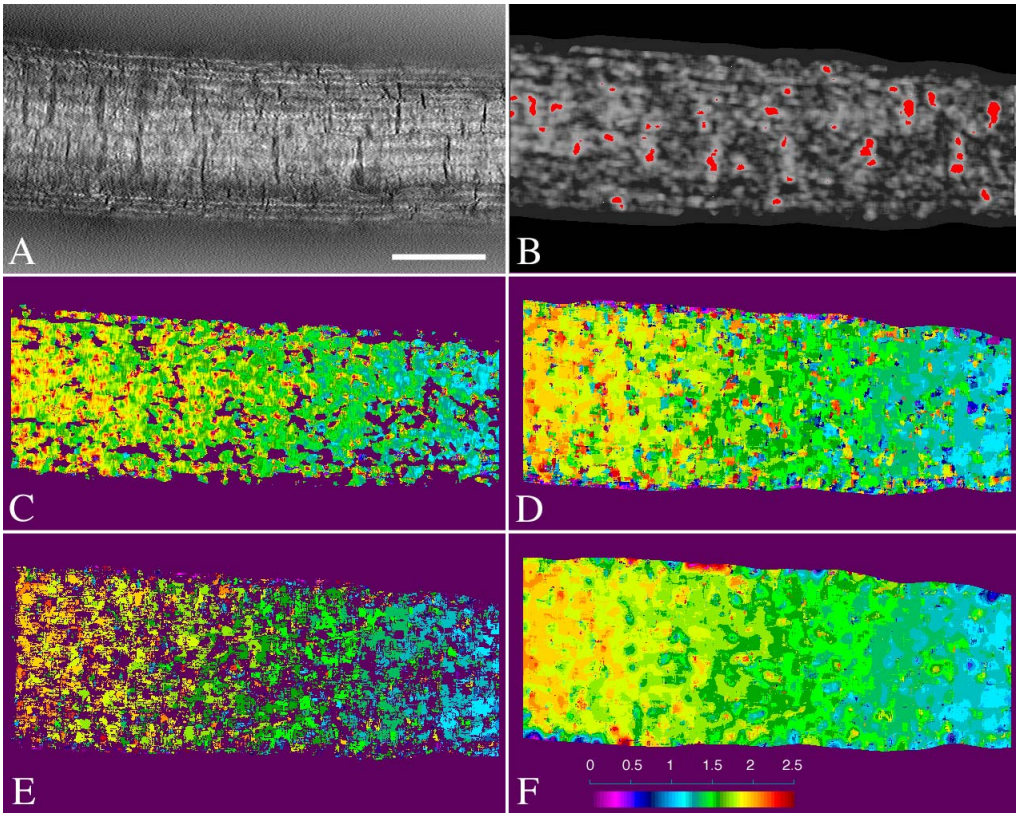

Figure 1. Steps in the robust tensor velocity estimation algorithm (see text) and [52].

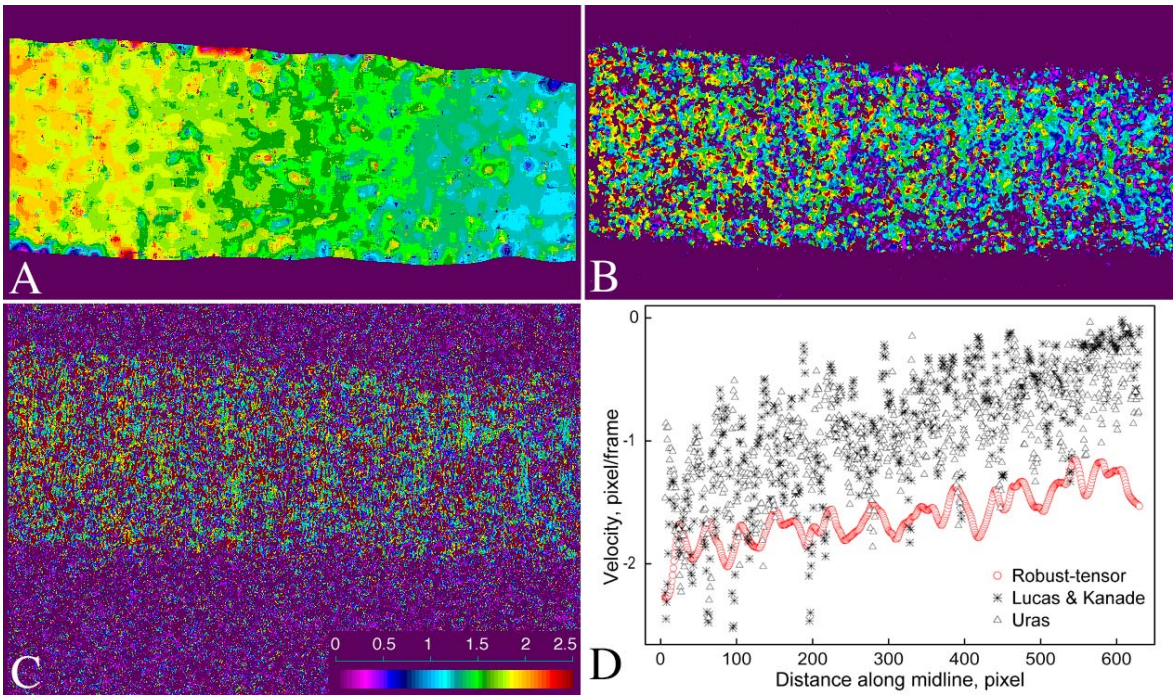

Figure 2. Comparison of our robust-tensor algorithm to two other optic flow-based motion estimation algorithms shows less varianced and higher accuracy of the robust tensor method compared to Lucas-Kanade and Uras algorithms.